JACS
JOURNAL OF THE AMERICAN CHEMICAL SOCIETY

COMMUNICATION

pubs.acs.org/JACS

Solution-Shear-Processed Quaterrylene Diimide Thin-Film Transistors Prepared by Pressure-Assisted Thermal Cleavage of Swallow Tails

Joon Hak Oh,[†,‖] Wen-Ya Lee,[†,⊥] Torsten Noe,[‡] Wen-Chang Chen,[⊥] Martin Könemann,[*,‡] and Zhenan Bao[*,†]

[†]Department of Chemical Engineering, Stanford University, Stanford, California 94305, United States
[‡]BASF SE, 67056 Ludwigshafen, Germany
[‖]School of Nano-Bioscience and Chemical Engineering, Ulsan National Institute of Science & Technology, Ulsan 689-798, Korea
[⊥]Department of Chemical Engineering, National Taiwan University, Taipei, Taiwan

Supporting Information

ABSTRACT: A scalable synthesis of swallow-tailed quaterrylene diimides (STQDIs) and a method for the solution processing of sparingly soluble quaterrylene diimide (QDI) thin films are described. The pressure-assisted thermal cleavage of swallow tails yields crystalline QDI layers with electron mobility up to 0.088 cm^2 V^{-1} s^{-1}. The developed method opens up a new route toward the solution processing of higher rylene diimides with poor solubility.

Rylene diimides have received much attention in dye chemistry,[1] supramolecular assemblies,[2] and optoelectronic applications[3] due to their chemical and photochemical stability as well as property tunability.[4] Compared to naphthalene diimides (NDIs)[5] and perylene diimides (PDIs),[6,7] whose absorption wavelengths are limited in the visible region, quaterrylene diimides (QDIs) have near-infrared (NIR) absorbing characteristics with a high extinction coefficient ($\sim 10^5$ M^{-1} cm^{-1}).[8,9] Expansion of conjugation along the long molecular axis from NDI to QDI raises the highest occupied molecular orbital (HOMO) level significantly, while the lowest unoccupied molecular orbital (LUMO) level is not affected substantially.[10] Using Marcus theory, Feng et al. found that, although the maxima of the overlap integral may decrease with the increase of the polyaromatic hydrocarbon core size, the overall hopping rate increases owing to the simultaneous decrease of the reorganization energy.[11]

The above features make QDIs suitable for a wide range of applications such as solar cells, NIR photodetectors, heat blockers, laser welding or marking of polymers, noninvasive imaging probes, IR photography, electrogenerated chemiluminescence labels, and single-molecule field-effect transistors.[12] Nevertheless, they have been far less employed for device applications because of the very high sublimation temperature and extremely low solubility. The substitution of branched alkyl chains at the imide position has been demonstrated not only to increase solubility but also to lower the temperature of the liquid crystalline phase for enabling facile processing.[4,13] However, these nonconjugated substituents reduce the density of chromophores and disturb the π-stacking, resulting in a low charge carrier mobility. Therefore, it is desirable to remove these substituents in a postprocessing step. One promising approach to this end is the thermal cleavage of solubilizing groups, which was used in photoresists,[14] soluble small-molecule derivatives of pentacene,[15] oligothiophene,[16] and porphyrin[17] as well as in polymers such as polyacetylene,[18] polythiophene,[19] polyphenylenevinylene,[20] and benzothiadiazole/pyrrole-based polymers.[21] Recently, thermally cleavable groups have been used for PDIs.[22] However, the removal of bulky pendant groups often causes void spaces and high surface roughness in the annealed film, and careful control of process conditions is required to optimize the performance.[23] Furthermore, although the electrical performance of several swallow-tailed rylene diimides was reported,[24,25] to our knowledge, there is no report on the successful fabrication of devices from sparingly soluble QDI derivatives with no substituent or a low degree of alkyl or aryl substitution, which are more desirable for high-performance applications.

Herein, we describe a scalable synthesis of soluble QDI derivatives and a solution-based approach to the fabrication of high-performance n-channel organic thin-film transistors (OTFTs) based on crystalline QDI thin films. Two swallow-tailed QDIs (namely, STQDIs: see Scheme 1) were synthesized and solution processed to form thin films by solution shearing[26] or spin coating. In the solution shearing, a small volume of an organic semiconductor solution is sandwiched between two preheated silicon wafers that move relative to each other at a controlled speed (Figure 1a). This method yields crystalline and aligned thin films from various soluble organic semiconductors.[26] It has been reported that **4** exhibits phase transition from plastic crystalline phase ($\mathrm{Col_p}$) to columnar hexagonal ordered liquid crystalline phase ($\mathrm{Col_{ho}}$) at 188 °C (Table S1 and Figure S1 [Supporting Information {SI}]).[4] However, thermal cleavage of the swallow tails was not reported. We found that the thermal cleavage of the swallow tails of the STQDIs takes place at a relatively lower temperature ranging from 350 to 400 °C. A very clean conversion to an ordered crystalline QDI layer was found. n-Channel OTFTs were produced by the approach of cleaving off solublizing R groups. The crystallinity of the resulting thin films could be further enhanced by pressure-assisted thermal cleavage, that is, a modified annealing technique with a flat substrate pressed on the film during the thermal cleavage (Figure 1b). This method also prevents film dewetting commonly observed for a

Received: November 22, 2010
Published: March 04, 2011

Scheme 1. Synthesis of STQDIs

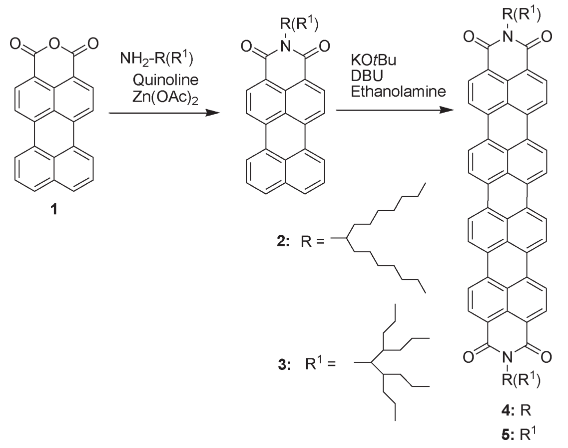

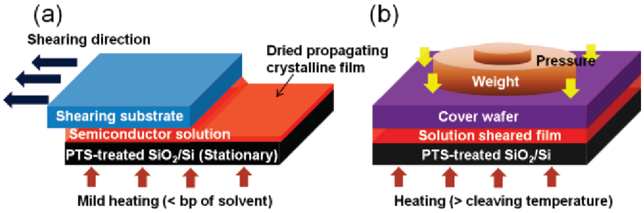

Figure 1. Schematic diagrams for (a) solution shearing and (b) pressure-assisted thermal cleavage.

high-temperature annealing[24] and improves the uniformity of the device performance. It was reported that drop-cast **4** thin films exhibit ambipolarity with the balanced hole and electron mobilities of about 1×10^{-3} cm^2 V^{-1} s^{-1}.[25] After the thermal annealing at 100 °C, the hole conduction disappeared, and the electron mobility decreased by an order of magnitude due to the increased trapping by the morphological change.[25,27,28] In this study, we significantly improved the electron mobility of QDI-based TFTs up to 0.088 cm^2 V^{-1} s^{-1}, through the pressure-assisted thermal cleavage of the solution-processed STQDI thin films. Our approach demonstrates a new route toward the solution processing of QDIs and can be expanded to the fabrication of other sparingly soluble rylene diimide thin films.

The synthesis of **5** has not been reported previously. The synthesis of **4** analogue ($R = CH(C_6H_{13})_2$) was reported by Langhals et al. in one step with a yield of 4% using a KOH melt at 300 °C.[9] Müllen et al. synthesized **4** in four steps with an overall yield of 46% from perylene-3,4-dicarboxylic monoimide **2** (PMI).[4] The base-induced dimerization of PMIs to QDIs using potassium-*tert*-butoxide (KO*t*Bu) was described earlier,[29] but only for aryl-substituted compounds which are more stable toward base-induced saponification compared to swallow-tailed R groups. A one-step base-induced dimerization of PMIs to QDIs using sodium-*tert*-butoxide (NaO*t*Bu) was proposed;[27] however, no demonstration has been reported. Here we synthesized **4** with a yield of 30% via a modified "green route"[29,30] in mild basic conditions using 8-diazabicyclo[5.4.0]undec-7-ene (DBU) and ethanolamine. We replaced 1,5-diazabicyclo[4.3.0]non-5-ene (DBN) used in ref 30 with the more readily available DBU.

Starting from perylene-3,4-dicarboxylic monoanhydride (**1**), the imidization was carried out using a standard procedure in quinoline with zinc acetate as the catalyst (Scheme 1). Yields of 66% and 34% were obtained for the less branched and more branched amines, respectively. Sterical reasons could account for the difference in yield. The base-induced dimerization of PMIs using KO*t*Bu, DBU, and ethanolamine yielded 30% and 23% of **4** and **5**, respectively. Our synthetic approach describes the first synthesis applicable to the industrial-scale production of these materials.

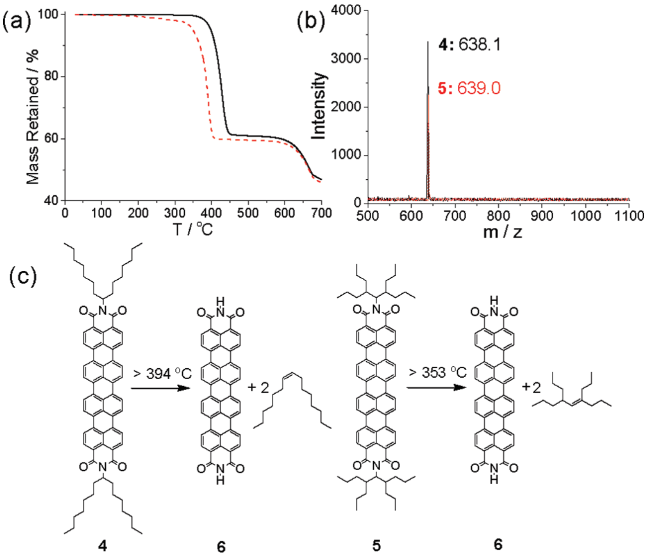

Figure 2. (a) Thermogravimetric analysis of STQDIs. The thermal cleavage of **5** (red dashed line) takes place at a temperature lower than that of **4** (black solid line) by about 40 °C. The second weight loss above 650 °C is due to the decomposition of QDI **6**. (b) MALDI-TOF MS spectra of **4** (black solid line) and **5** (red dashed line) after annealing at 400 and 370 °C for 1 h, respectively. (c) The thermal cleavage mechanism of STQDIs.

The thermal cleavage of the swallow tails of **4** and **5** took place at 394 and 353 °C, respectively, as shown in Figure 2a. The mass loss was approximately 40%, which corresponds well to the loss of the two alkyl chains. Mass spectrometry (MS) analyses on the residues after the thermogravimetry analysis (TGA) of **4** and **5** showed strong peaks respectively at 638.1 and 639.0 g$\cdot$mo1^{-1} (Figure 2b), which agrees well with the molecular weight (638.6 g$\cdot$mo1^{-1}) of **6**. Whereas Würthner et al. described the cleavage of branched groups from rylene diimides by using strong Lewis acid BBr_3 in a nonquantitative yield,[31] we found that the thermal cleavage of STQDIs surprisingly leads to a very clean conversion to materials with semiconductor-grade purity without the use of chemical reagents in a short reaction time (<1 h). In order to lower the cleaving temperature of **4**, 4,6-dipropylnon-5-yl-amine that provides highly substituted and more stable olefin upon thermal cleavage was used for **5** (Figure 2c).

UV−vis spectra of pristine **6** and annealed **4** at 420 °C exhibited similar absorptions in sulfuric acid with the identical λ_{max} of 872 nm and the very high extinctions in the NIR region (see Figure S2 [SI]), indicating that there is no visible degradation due to the thermal annealing. Spin-coated thin films of **4** and **5** showed a long absorption wavelength up to ∼1000 nm with λ_{max} of 688 and 707 nm, respectively (Figure S3 [SI]). After thermal cleavage, the absorption edge exhibited a bathochromic shift of 150 nm, indicating a very small band gap of ∼1.1 eV. The broader absorption range of the annealed STQDI films indicates that the thermal cleavage not only removes the alkyl chains but also enhances $\pi-\pi$ stacking of the molecules, i.e. the aggregation of **6** chromophores. Ultraviolet photoelectron spectroscopy

Table 1. **Electronic and OTFT Characteristics of Solution-Sheared STQDI Thin Films**

cmpd	annealing[a]	λ_{max} [nm]	E_g [eV]	μ [cm^2 V^{-1} s^{-1}]	I_{on}/I_{off}	V_t [V]
4	before	684	1.3	2.9×10^{-5}	2.3×10^{3}	−19
5	before	705	1.3	1.1×10^{-4}	8.8×10^{3}	5
4	after	597	1.1	0.088	2.5×10^{3}	−1.8
5	after	609	1.1	0.061	4.9×10^{4}	−0.5

[a] The annealings of **4** and **5** were performed at 400 and 370 °C for 1 h under the pressure of 10 and 20 kPa, respectively.

(UPS) revealed the HOMO levels of −5.4 to −5.6 eV for the annealed films. This means the LUMO levels of the annealed films correspond to −4.3 to −4.5 eV, which are located in the empirical LUMO range for air-stable n-channel operation.[6]

To investigate the effects of thermal cleavage on the charge transport, top-contact OTFTs were fabricated with a SiO_2 (300 nm)/n-doped Si wafer with the surface modification layer of phenyltrichlorosilane (PTS). The as-prepared OTFTs before annealing showed electron mobility (μ) ranging from 10^{-4} to 10^{-5} cm^2 V^{-1} s^{-1}, whereas after the thermal cleavage they yielded 2−3 orders of magnitude higher μ up to 0.088 cm^2 V^{-1} s^{-1}. This indicates that the thermal cleavage of the branched chains indeed facilitates the molecular packing and thus improves charge transport. The optimized annealing temperatures of **4** and **5** were 400 and 370 °C, respectively. The solution-sheared thin films typically yielded 1 order of magnitude higher μ compared to that by spin-coated thin films under pressure, due to their aligned and crystalline nature. The optimized performance of solution-sheared OTFTs and the annealing conditions are listed in Table 1 (for the performance details, see Table S2 and Figure S4 [SI]). The STQDI TFTs were not as air-stable as other rylene diimides with similarly low-lying LUMOs.[6] In addition, the solution-sheared OTFTs showed relatively higher air stability with the same order of magnitude mobility after exposure to air for a week, while the spin-coated devices degraded more rapidly with about 1 order of magnitude decrease (Figure S5 [SI]). The solution-sheared thin films benefit from the kinetic factors due to the larger crystalline grains. This is consistent with our recent finding that the film thickness and morphology also impact the air stability in addition to the LUMO level of the molecule.[32]

The out-of-plane X-ray diffraction (XRD) measurements of **5** thin films annealed at 370 °C exhibited a sharp primary peak at $2\theta = 3.54°$ (Figure S6 [SI]). This corresponds to a d(001)-spacing of 24.94 Å, close to the geometry-optimized molecular length of **6** (23.7 Å).[33] This result indicates that the molecules adopt an edge-on orientation in the thin films and have favorable molecular orientations for charge transport between source-to-drain electrodes. The morphology of as-annealed thin films showed some portions of a void area and a high roughness (Figures S7 and S8 [SI]), thereby giving rise to some device-to-device variations. However, the pressure-assisted thermal cleavage substantially improved the performance and uniformity (Figure S9 [SI]). Upon annealing under a pressure of 20 kPa, the average mobilities of solution-sheared and spin-coated films of **5** were enhanced by 4−8 times compared to those prepared without pressure. The roughness of **5** thin films decreased significantly from 12.8 nm, down to 6.7 nm for 10 kPa and 5.7 nm for 20 kPa (Figure S10 [SI]). The applied pressure suppressed the 3D growth of the grains and forced the grains to coalesce, leading to less empty space and enhanced mobility.

Intriguingly, we found that the surface treatment of the cover wafer for pressing plays an important role in the performance of the resulting devices. A PTS-treated cover wafer exhibited higher μ, compared to the bare or *n*-octadecyltrimethoxysilane (OTS)-treated one (Figure S11 [SI]). This is presumably related to the difference in the wetting properties of the molecules on the surface, which affects molecular reorganization during the annealing (Figure S12 [SI]).

In summary, we developed a scalable synthesis of soluble QDIs and demonstrated a solution fabrication of crystalline, NIR-absorbing QDI thin films. The swallow tails were used as the solubilizing agent for the insoluble QDI moiety and could be subsequently removed by thermal treatment at temperatures ranging from 350 to 400 °C, sufficiently low to provide QDI **6** without degradation. The pressure-assisted thermal cleavage significantly reduced the surface roughness and void space of the resulting films, leading to μ up to 0.088 cm^2 V^{-1} s^{-1}. The developed method opens up a new route toward the solution-based fabrication of the crystalline thin films of sparingly soluble higher rylene diimides.

■ ASSOCIATED CONTENT

Ⓢ Supporting Information. Experimental details, OTFT data, UV−vis spectra, XRD data, optical microscope images, and AFM images. This material is available free of charge via the Internet at http://pubs.acs.org.

■ AUTHOR INFORMATION

Corresponding Author

martin.koenemann@basf.com; zbao@stanford.edu

■ ACKNOWLEDGMENT

This work was supported by BASF SE and the Sloan Research Fellowship. J.H.O. acknowledges partial financial support from Basic Science Research Program through the National Research Foundation of Korea (NRF) funded by the Ministry of Education, Science and Technology (Grant No. 2010-0025292).

■ REFERENCES

(1) Hunger, K. *Industrial Dyes: Chemistry, Properties, Applications*; Wiley-VCH: Weinheim, 2003; Vol. 1.

(2) Würthner, F. *Chem. Commun.* **2004**, 1564–1579.

(3) Schmidt-Mende, L.; Fechtenkotter, A.; Müllen, K.; Moons, E.; Friend, R. H.; MacKenzie, J. D. *Science* **2001**, *293*, 1119–1122.

(4) Nolde, F.; Pisula, W.; Müller, S.; Kohl, C.; Müllen, K. *Chem. Mater.* **2006**, *18*, 3715–3725.

(5) Oh, J. H.; Suraru, S.-L.; Lee, W.-Y.; Könemann, M.; Höffken, H. W.; Röger, C.; Schmidt, R.; Chung, Y.; Chen, W.-C.; Würthner, F.; Bao, Z. *Adv. Funct. Mater.* **2010**, *20*, 2148–2156.

(6) Jones, B. A.; Facchetti, A.; Wasielewski, M. R.; Marks, T. J. *J. Am. Chem. Soc.* **2007**, *129*, 15259–15278.

(7) Oh, J. H.; Lee, H. W.; Mannsfeld, S.; Stoltenberg, R. M.; Jung, E.; Jin, Y. W.; Kim, J. M.; Yoo, J.-B.; Bao, Z. *Proc. Natl. Acad. Sci. U.S.A.* **2009**, *106*, 6065–6070.

(8) (a) Quante, H.; Müllen, K. *Angew. Chem., Int. Ed.* **1995**, *34*, 1323–1325. (b) Adachi, M.; Nagao, Y. *Chem. Mater.* **2001**, *13*, 662–669. (c) Lee, S. K.; Zu, Y.; Herrmann, A.; Geerts, Y.; Müllen, K.; Bard, A. J. *J. Am. Chem. Soc.* **1999**, *121*, 3513–3520.

(9) Langhals, H.; Schönmann, G.; Feiler, L. *Tetrahedron Lett.* **1995**, *36*, 6423–6424.

(10) Lee, S. K.; Zu, Y.; Herrmann, A.; Geerts, Y.; Müllen, K.; Bard, A. J. *J. Am. Chem. Soc.* **1999**, *121*, 3513–3520.

(11) Feng, X.; Marcon, V.; Pisula, W.; Hansen, M. R.; Kirkpatrick, J.; Grozema, F.; Andrienko, D.; Kremer, K.; Müllen, K. *Nat. Mater.* **2009**, *8*, 421–426.

(12) (a) Fabian, J.; Nakazumi, H.; Matsuoka, M. *Chem. Rev.* **1992**, *92*, 1197–1226. (b) Zhao, W.; Carreira, E. M. *Angew. Chem., Int. Ed.* **2005**, *44*, 1677–1679.

(13) (a) Wicklein, A.; Lang, A.; Muth, M.; Thelakkat, M. *J. Am. Chem. Soc.* **2009**, *131*, 14442–14453. (b) Prehm, M.; Liu, F.; Zeng, X.; Ungar, G.; Tschierske, C. *J. Am. Chem. Soc.* **2008**, *130*, 14922–14923.

(14) Fréchet, J. M. J.; Eichler, E.; Ito, H.; Willson, C. G. *Polymer* **1983**, *24*, 995–1000.

(15) (a) Herwig, P. T.; Müllen, K. *Adv. Mater.* **1999**, *11*, 480–483. (b) Afzali, A.; Dimitrakopoulos, C. D.; Breen, T. L. *J. Am. Chem. Soc.* **2002**, *124*, 8812–8813.

(16) Murphy, A. R.; Fréchet, J. M. J.; Chang, P.; Lee, J.; Subramanian, V. *J. Am. Chem. Soc.* **2004**, *126*, 1596–1597.

(17) Aramaki, S.; Sakai, Y.; Ono, N. *Appl. Phys. Lett.* **2004**, *84*, 2085–2087.

(18) Edwards, J. H.; Feast, W. J.; Bott, D. C. *Polymer* **1984**, *25*, 395–398.

(19) Liu, J.; Kadnikova, E. N.; Liu, Y.; McGehee, M. D.; Fréchet, J. M. J. *J. Am. Chem. Soc.* **2004**, *126*, 9486–9487.

(20) Wagaman, M. W.; Grubbs, R. H. *Macromolecules* **1997**, *30*, 3978–3985.

(21) Edder, C.; Armstrong, P. B.; Prado, K. B.; Fréchet, J. M. J. *Chem. Commun.* **2006**, 1965–1967.

(22) Ando, S.; Facchetti, A.; Marks, T. J. *Org. Lett.* **2010**, *12*, 4852–4855.

(23) Chang, P. C.; Lee, J.; Huang, D.; Subramanian, V.; Murphy, A. R.; Fréchet, J. M. J. *Chem. Mater.* **2004**, *16*, 4783–4789.

(24) Liu, C.; Liu, Z.; Lemke, H. T.; Tsao, H. N.; Naber, R. C. G.; Li, Y.; Banger, K.; Müllen, K.; Nielsen, M. M.; Sirringhaus, H. *Chem. Mater.* **2010**, *22*, 2120–2124.

(25) Tsao, H. N.; Pisula, W.; Liu, Z.; Osikowicz, W.; Salaneck, W. R.; Müllen, K. *Adv. Mater.* **2008**, *20*, 2715–2719.

(26) Becerril, H. A.; Roberts, M. E.; Liu, Z.; Locklin, J.; Bao, Z. *Adv. Mater.* **2008**, *20*, 2588–2594.

(27) Avlasevich, Y.; Li, C.; Müllen, K. *J. Mater. Chem.* **2010**, *20* 3814–3826.

(28) Schmaltz, B.; Weil, T.; Müllen, K. *Adv. Mater.* **2009**, *21* 1067–1078.

(29) Könemann, M.; Böhm, A.; Bidlingmaier, H.; Rieger, R.; Blaschka, P.; Reichelt, H.; Krieger, M. U.S. 7,741,487, 2010.

(30) Sakamoto, T.; Pac, C. *J. Org. Chem.* **2000**, *66*, 94–98.

(31) Wang, H.; Kaiser, T. E.; Uemura, S.; Würthner, F. *Chem. Commun.* **2008**, 1181–1183.

(32) Oh, J. H.; Sun, Y.-S.; Schmidt, R.; Toney, M. F.; Nordlund, D.; Könemann, M.; Würthner, F.; Bao, Z. *Chem. Mater.* **2009**, *21*, 5508–5518.

(33) Wagner, C.; Franke, R.; Dienel, T.; Forker, R.; Jacob, R.; Fritz, T. *Appl. Phys. Lett.* **2007**, *91*, 113111.